Model Investigations for Vanadium−Protein Interactions. Synthetic, Structural, and Physical Studies of Vanadium(III) and Oxovanadium(IV/V) Complexes with Amidate Ligands

Anastasios D. Keramidas,[1a] Aggelos B. Papaioannou,[1a] Antonis Vlahos,[1a] Themistoklis A. Kabanos,*[,1a] George Bonas,[1b] Alexandros Makriyannis,[1b] Cathrin P. Rapropoulou,[1c] and Aris Terzis[1c]

Department of Chemistry, Section of Inorganic and Analytical Chemistry, University of Ioannina, 45110 Ioannina, Greece, Institute of Organic and Pharmaceutical Chemistry, National Hellenic Research Foundation, 48 Vas. Constantinou Ave., 116 35 Athens, Greece, and NRPCS Demokritos, Institute of Materials Science, 15310 Aghia Paraskevi Attikis, Greece

Received March 31, 1995[⊗]

Reaction of the amide ligand *N*-[2-((2-pyridylmethylene)amino)phenyl]pyridine-2-carboxamide (Hcapca) with VCl_3 affords the compound *trans*-[VCl_2(capca)] (**1**), the first example of a vanadium(III) complex containing a vanadium-deprotonated amide nitrogen bond, while reaction of bis(pentane-2,4-dionato)oxovanadium(IV) with the related ligands *N*-[2-((2-phenolylmethylene)amino)phenyl]pyridine-2-carboxamide (H_2phepca), 1-(2-hydroxybenzamido)-2-(2-pyridinecarboxamido)benzene (H_3hypyb), and 1,2-bis(2-hydroxybenzamido)benzene (H_4hybeb) yields the complexes [VO(phepca)] (**2**), Na[VO(hypyb)]·2CH_3OH (**4**·2CH_3OH), and Na_2[VO(hybeb)]·3CH_3OH (**5**·3CH_3OH) respectively. The preparation of the complex {*N*-[2-((2-thiophenoylmethylene)amino)phenyl]pyridine-2-carboxamido}oxovanadium(IV) (**3**) has been achieved by reaction of *N*-(2-aminophenyl)pyridine-2-carboxamide and 2-mercaptobenzaldehyde with $[VO(CH_3COO)_2]_x$. Oxidation of complex **5**·3CH_3OH with silver nitrate gives its vanadium(V) analogue (**8**·CH_3OH), which is readily converted to its corresponding tetraethylammonium salt (**10**·CH_2Cl_2) by a reaction with Et_4NCl. The crystal structures of the octahedral **1**·CH_3CN, and the square-pyramidal complexes **3**, **4**·CH_3CN, **5**·2CH_3OH, and **10** were demonstrated by X-ray diffraction analysis. Crystal data are as follows: **1**·CH_3CN, $C_{18}H_{13}Cl_2N_4OV$·CH_3CN M_r = 464.23, monoclinic, $P2_1/n$, a = 10.5991(7) Å, b = 13.9981(7) Å, c = 14.4021(7) Å, β = 98.649(2)°, V = 2112.5(3) Å^3, Z = 4, R = 0.0323, and R_w 0.0335; **3**, $C_{19}H_{13}N_3O_2SV$, M_r = 398.34, monoclinic, $P2_1$/n, a = 12.1108(10) Å, b = 19.4439(18) Å, c = 7.2351(7) Å, β = 103.012(3)°, V = 1660.0(4) Å^3, Z = 4, R = 0.0355, and R_w = 0.0376; **4**·CH_3CN, $C_{19}H_{12}N_3O_4VNa$·CH_3CN, M_r = 461.31, monoclinic, $P2_1$/c, a = 11.528(1) Å, b = 11.209(1) Å, c = 16.512(2) Å, β = 103.928(4)°, V = 2071.0(5) Å^3, Z = 4, R = 0.0649, and R_w = 0.0806; **5**·2CH_3OH, $C_{20}H_{10}N_2O_5VNa_2$·2CH_3OH, M_r = 519.31, triclinic, $P1$, a = 12.839(1) Å, b = 8.334(1) Å, c = 12.201(1) Å, α = 106.492(2)°, β = 105.408(2)°, γ = 73.465(2)°, V = 1175.6(3) Å^3, Z = 2, R = 0.0894, and R_w = 0.1043; **10**, $C_{28}H_{32}N_3O_5V$ M_r = 541.52, monoclinic, $P2_1$/c, a = 11.711(3) Å, b = 18.554(5) Å, c = 12.335(3) Å, β = 95.947(9)°, V = 2666(2) Å^3, Z = 4, R = 0.0904, and R_w = 0.0879. In addition to the synthesis and crystallographic studies, we report the optical, infrared, magnetic, and electrochemical properties of these complexes. Electron paramagnetic resonance [of oxovanadium(IV) species] and ^{1}H, ^{13}C{^{1}H}, and ^{51}V nuclear magnetic resonance [of oxovanadium(V) complex] properties are reported as well. This study represents the first systematic study of vanadium(III), $V^{IV}O^{2+}$, and $V^{V}O^{3+}$ species containing a vanadium-deprotonated amide nitrogen bond.

Introduction

There is currently an explosive development in the coordination chemistry and biochemistry of vanadium.[2] This is mainly due to the discovery that vanadium is an essential element in biological systems, participating in enzymic reactions such as bromination of a variety of organic substrates[3] and nitrogen fixation,[4] as well as to vanadium's insulinomimetic properties[5] and in particular the recent promising human clinical trials of oral treatment of diebetes[5c] by sodium metavanadate and oxovanadium (VO^{2+}) species. In addition, vanadate has shown great utility as a tool in molecular biology for recognizing and understanding the structure of phosphate binding proteins, by catalytic photocleavage of the peptide backbone.[6]

It is obvious from all these and many other biological implications of vanadium, that the exploration of interaction of vanadium with potential metal ion binding sites on proteins is very important. The binding of a metal atom by a protein may

* Author to whom correspondence should be addressed.

⊗ Abstract published in *Advance ACS Abstracts,* November 15, 1995.

(1) (a) University of Ioannina. (b) National Hellenic Research Foundation. (c) Institute of Material Science.

(2) (a) *Vanadium in Biological Systems*; Chasteen, N. D., Ed.; Kluwer Academic Publishers: Dordrecht, The Netherlands, 1990. (b) Butler, A.; Carrano, C. J. *Coord. Chem. Rev.* **1991**, 109, 61. (c) Rehder, D. *Angew. Chem., Int. Ed. Engl.* **1991**, 301, 148. (d) Butler, A.: Clague, M. J.; Meister, G. E. *Chem. Rev.* **1994**, 94, 625.

(3) (a) Butler, A.; Walker, J. V. *Chem. Rev.* **1993**, 93, 1937. (b) *Bioinorganic Catalysis*; Reedijk, J.; Ed.; Marcel Dekker, Inc.: New York, 1993; pp 425−445.

(4) Chisnell, J. R.; Premakumar, R.; Bishop, P. E. *J. Bacteriol.* **1988**, 170, 27.

(5) (a) McNeill, J. H.; Yuen, V. G.; Hoveyda, H. R.; Orving, C. *J. Med. Chem.* **1992**, 35, 1491. (b) Cam, M. C.; Pederson, R. A.; Brownsey, R. W.; McNeil, J. H. *Diabetologia* **1993**, 36, 218. (c) Symposium Proceedings of the "Vanadium" Symposium, July 28−30, 1994: "Biochemistry, Physiology and Therapy of Vanadium in Diabetes", appearing as a special volume of *Cell. Mol. Biochem.*, in press.

(6) (a) Cremo, C. R.; Long,g. T.; Grammer, J. C. *Biochemistry* **1990**, 29, 7982. (b) Muhlrad, A.; Peyser, M. Y.; Ringel, I. *Biochemistry* **1991**, 30, 958. (c) Cremo C. R.; Loo, J. A.; Edmonds, C. G.; Hatlelid, K. M. *Biochemistry* **1992**, 31, 491.

0020-1669/96/1335-0357$12.00/0

principally involve ionizable side chains and the −NHCO− groups of the peptide chain backbone. To date, there are only a very few structurally characterized[7−10] examples and solution (water) studies[11−13] as well in the literature concerning the interaction of vanadium with the amide(peptide) functionality. Herein we report the interaction of vanadium in oxidation states III, IV, and V with the −CON⁻− functionality, the first structural characterization of such a vanadium(III) complex, and also the structural characterization of oxovanadium(IV/V) species with amidate and diamidate polyanionic chelating ligands, continuing our program concerning the preparation and characterization of vanadium compounds with amino acids and small oligopeptides (or peptide-like molecules). In addition, the optical, infrared, magnetic, and electrochemical properties of the complexes are reported. Electron paramagnetic resonace[14] [of oxovanadium(IV) species] and ^{1}H, ^{13}C{^{1}H}, ^{51}V nuclear magnetic resonace [of oxovanadium(V) complex] properties are reported as well. A preliminary report of this research has been communicated previously.[7c,d]

Experimental Section

Materials. Bis(triphenylphosphoranylidene)ammonium chloride, $[(Ph_3P)_2N]Cl$, was bought from Aldrich and was used as received. Bis(pentane-2,4-dionato)oxovanadium(IV), $[VO(acac)_2]$,[15] bis(acetato)oxovanadium(IV), $[VO(CH_3COO)_2]_x$,[16] *o*-aminobenzaldehyde,[17] 2-mercaptobenzaldehyde,[18] *N*-(2-aminophenyl) pyridine-2-carboxamide,[7b] and tetraethylammonium perchlorate[7b] were prepared by literature procedures. The purity of the above molecules (except of Hmeba which was not isolated) was confirmed by elemental analyses (C, H, N, and V, for vanadium complexes) and infrared spectroscopy. Merck silica gel 60 F254 TLC plates were used for thin layer chromatography. Reagent grade dichloromethane, acetonitrile, triethylamine, and nitromethane were dried and distilled over powdered calcium hydride, while toluene, dioxane, and diethyl ether were dried and distilled over sodium wire. Methanol was dried by refluxing over magnesium methoxide. Synthesis, distillations, crystallization of the complexes, and spectroscopic characterization were performed under high-purity argon using standard Schlenk techniques.

C, H, N, and S analyses were conducted by the University of Ioannina's microanalytical service, vanadium was determined gravimetrically as vanadium pentoxide or by atomic absorption and chloride analyses were carried out by potentiometric titration.

***N*-[2-((2-Pyridylmethylene)amino)phenyl]pyridine-2-carboxamide (Hcapca).** A solution of methanol (70 mL) containing Hpyca (10.00 g, 46.9 mmol) and 2-pyridinecarboxaldehyde (5.03 g, 47.0 mmol) was refluxed overnight. The solution was cooled at −10 °C for 2 h, and the resulting yellow precipitate was filtered off, washed with diethyl ether (3 × 20 mL), and dried in vacuo. The product was recrystallized from methanol. Yield: 9.20 g (65%). Mp: 116−117 °C. Anal. Calcd for $C_{18}H_{14}N_4O$: C, 71.51; H, 4.67; N, 18.53. Found: C, 71.70; H, 4.70; N, 18.50. ^{1}H NMR: δ 7.15 (dd, J = 8.4 Hz, 7.6 Hz, 1H), 7.33−7.42 (m, 3H), 7.42−7.49 (m, 1H), 7.83−7.89 (m, 2H), 8.30 [d, J = 7.9 Hz, 1H, *H*−C(15)[19a]], 8.56 [d, J = 7.9 Hz, 1H, *H*−C(4)], 8.65 [d, J = 4.6 Hz, 1H, *H*−C(18)], 8.68−8.77 (m, 2H), 8.79 [s, 1H, Ph−N=C(6)−*H*], 11.60 [br s, 1H, −CON*H*−]. ^{13}C{^{1}H} NMR: δ 116.28, 119.47, 121.63, 122.31, 123.90, 125.21, 126.22, 128.86, 134.19 [quat, *C*(12)[19a] or *C*(7)], 136.59, 137.50, 137.58 [quat, *C*(12) or *C*(7)], 148.13, 149.64, 150.45 [quat, *C*(14)], 154.78 [quat, *C*(5)], 158.40 [*C*(6)], 161.75 [quat, *C*(13)]. MS: *m/e* 302 [M]. R_f = 0.16 (4:1 chloroform/*n*-hexane).

***N*-[2-((2-Phenolylmethylene)amino)phenyl]pyridine-2-carboxamide (H_2phepca).** A methanol solution (100 mL) containing Hpyca (3.500 g, 16.41 mmol) and salicylaldehyde (2.200 g, 18.02 mmol) was refluxed for 1 h. The yellow solid which formed was filtered off and washed with diethyl ether (2 × 20 mL). The solid was recrystallized from toluene. Yield: 4.75 g (91%). Mp: 178−179 °C. Anal. Calcd for $C_{19}H_{15}N_3O_2$: C, 71.91; H, 4.76; N, 13.24; Found: C, 71.88; H, 4.75; N, 13.20. ^{1}H NMR: δ 6.99 (dd, J = 7.9, 7.3 Hz, 1H), 7.10 (d, J = 8.6 Hz, 1H), 7.14−7.29 (m, 2H), 7.32-7.42 (m, 1H), 7.42−7.53 (m, 2H), 7.88 (dd, J = 8.6, 7.9 Hz, 1H), 8.27 [d, J = 7.9 Hz, 1H, *H*−C(16)[19a]], 8.67 (d, J = 7.3 Hz, 2H), 8.71 [s, 1H, C(7)−*H*], 10.97 [br s, 1H, C(1)−O*H*], 12.26 [s, 1H, −CON*H*]. ^{13}C{^{1}H} NMR: δ 117.43, 118.01, 119.40, 119.50 [quat, *C*(6)[19a]], 120.24, 122.10, 124.48, 126.42, 128.06, 132.25 [quat, *C*(8) or *C*(13)], 133.01, 133.70, 137.54, 138.91 [quat, *C*-(8) or *C*(13)], 148.42, 149.97 [quat, *C*(15)], 161.03 [quat, *C*(1)], 162.04 [quat, −CON*H*−], 163.99 [−N = *C*H−]. MS: *m/e* 317 [M]. R_f = 0.32 (4:1 chloroform/*n*-hexane).

1-(2-Acetoxybenzamido)-2-(2-pyridinecarboxamido)benzene (H_2hypybe). To a stirred anhydrous dioxane (60 mL) solution of Hpyca (10.000 g, 46.90 mmol) was slowly added acetylsalicyloyl chloride (9.310 g, 46.90 mmol). After this mixture was stirred for 18 h, water (300 mL) was added dropwise to the stirred solution, and the resulting white precipitate was filtered off and washed with water (3 × 50 mL). The product was recystallized from methanol. Yield: 13.38 g (76%). Mp: 146.5−147.5 °C. Anal. Calcd for $C_{21}H_{17}N_3O_4$: C, 67.19; H, 4.56; N, 11.19. Found: C, 67.20; H, 4.60; N, 11.07. ^{1}H NMR: δ 2.26 (s, 3H, C*H*$_3$−COO−), 7.13 (d, J = 8.1 Hz, 1H), 7.21−7.34 (m, 3H), 7.41−7.51 (m, 2H), 7.61 (dd, J = 7.1, 2.2 Hz, 1H), 7,77 (d, J = 7.4 Hz, 1H), 7.82−7.91 (m, 2H), 8.22 [d, J = 7.5 Hz, 1H, *H*−C(16)[19a]], 8.56 [d, J = 4.6 Hz, 1H, *H*−C(19)], 9.05 (br s, 1H, Ph−CON*H*−), 10.20 [br s, 1H, Py−CON*H*−]. ^{13}C{^{1}H} NMR: δ 21.10(−*C*H$_3$), 122.65, 123.41, 123.83, 124.30, 125.99, 126.16, 126.25, 126.49, 126.78, 128.18 [quat, *C*(6)[19a]], 129.88, 130.25 [quat, *C*(8) or *C*(13)], 130.61 [quat, *C*(8) or *C*(13)], 132.09, 137.66, 148.30 [*C*(19)], 148.49 [quat, *C*(1)], 149.07 [quat, *C*(15)], 163.17 [quat, *C*(14)], 164.47 [quat, CH$_3$O*C*O−], 169.31 [quat, *C*(7)]. MS: *m/e* 375 [M]. R_f = 0.15 (4:1 chloroform/*n*-hexane).

1,2-Bis(2-acetoxybenzamido)benzene (H_2hybebe). The molecule was prepared in a fashion similar to that used for H_2hypybe, except 1,2-phenylenediamine was used instead of Hpyca. Yield: 71%. Mp: 159−160 °C. Anal. Calcd for $C_{24}H_{20}N_2O_6$: C, 66.66; H, 4.66; N, 6.48. Found: C, 66.70; H, 4.58; N, 6.50. ^{1}H NMR: δ 2.20 (s, 6H,

(7) (a) Kabanos, T. A.; Keramidas, A. D.; Terzis, A. *J. Chem. Soc., Chem. Commum.* **1990**, 1664. (b) Hanson, G. R.; Kabanos, T. A.; Keramidas, A. D.; Mentzafos, D.; Terzis, A. *Inorg. Chem.* **1992**, 31, 2587. (c) Kabanos, T. A.; Keramidas, A. D.; Papaioannou, A. B.; Terzis, A. *J. Chem. Soc., Chem. Commun.* **1993**, 643. (d) Terzis, A.; Kabanos, T. A.; Keramidas, A. D.; Papaioannou, A. B. Abstract-International Union of Crystallography, XVI Congress and General Assembly, Beijing, China, August 1993, p 224. (e) Kabanos, T. A.; Keramidas, A. D.; Papaioannou, A. B.; Terzis, A. *Inorg. Chem.* **1994**, 33, 845.
(8) Edema, J. J. H.; Meetsma, A.; Bolhuis, F.; Gambarotta, S. *Inorg. Chem.* **1991**, 30, 2056.
(9) Bovoric, A. S.; Dewey, T. M.; Raymond, K. N. *Inorg. Chem.* **1993**, 32, 413.
(10) Cornman, C. R.; Geiser-Bush, K. M.; Singh, P. *Inorg. Chem.* **1994**, 33, 4621.
(11) (a) Rehder, D.; Weideman, C.; Duch, A.; Priebsch, W. *Inorg. Chem.* **1988**, 27, 584. (b) Rehder, D. *Inorg. Chem.* **1988**, 27, 4312. (c) Rehder, D.; Holst, H.; Quaas, R.; Hinrichs, W.; Hahn, V.; Saenger, W. *J. Inorg. Biochem.* **1989**, 37, 141. (d) Rehder, D.; Holst, H.; Priebsch, W.; Vilter, H. *J. Inorg. Biochem.* **1991**, 41, 171. (e) Knuttel, K.; Muller, A.; Rehder, D.; Vilter, H,; Wittneber, V. *FEBS Lett.* **1992**, 301, 11.
(12) (a) Jaswal, J. S.; Tracey, A. S. *Can. J. Chem.* **1991**, 69, 1600. (b) Jaswal, J. S.; Tracey, A. S. *J. Am. Chem. Soc.* **1993**, 115, 5600.
(13) (a) Crans, D. C.; Bunch, R. L.; Theisen, L. A. *J. Am. Chem. Soc.* **1989**, 111, 7597. (b) Crans, D. C.; Holst. H.; Keramidas, A. D.; Rehder, D. *Inorg. Chem.* **1995**, 34, 2524.
(14) Abbreviations: CV, cyclic voltammetry; EPR, electron paramagnetic resonance; MS, mass spectrum; NMR, nuclear magnetic resonance, acac⁻, pentane-2,4-dionate; Hmeba, 2-mercaptobenzaldehyde; Hpyca, *N*-(2-aminophenyl)pyridine-2-carboxamide; H_2pycac, *N*-[2-(4-oxopent-2-en-2-ylamino)phenyl]pyridine-2-carboxamide; H_2salen, *N*,*N*′-ethylenebis(salicylideneamine); H_4depa-H, *N*,*N*′-bis(2-hydroxyphenyl)-2,2-diethylpropanediamide; H_4hymeb, 1,2-bis(2-hydroxy-2-methylpropanamido)benzene; H_2pycbac, *N*-[2-(4-phenyl-4-oxobut-2-en-2-ylamino)phenyl]pyridine-2-carboxamide.
(15) Rowe, R. A.; Jones, M. M. *Inorg. Synth.* **1957**, 5, 113.
(16) Chand-Paul, R.; Bathia, S.; Kumar, A. *Inorg. Synth.* **1982**, 13, 181.
(17) Smith, L. I.; Opie, J. W. *Organic Syntheses. Collective Volume 3*; Wiley: London, **1955**; p 56.
(18) Marini, P. J.; Murray, K. S.; West, B. O. *J. Chem. Soc., Dalton Trans.* **1983**, 143.
(19) (a) The numbering of the carbons for the ligands Hcapca, H_2phepca, H_3hypyb and H_4hybeb (and H_2hybebe) is the same as that reported in Figures 1, 2, 5, and 3 respectively. (b) ^{13}C resonances of the ring carbon attached to substituent shown.

−*C*H$_3$), 7.11 [d, J = 8.1 Hz, 2H, *H*−C(2)[19a] and *H*−C(19)], 7.14−7.21 (m, 2H), 7.27 (dd, J = 7.9, 7.6 Hz, 2H), 7.41−7.51 (m, 4H), 7.75 [d, J = 7.4 Hz, 2H, *H*−C(5) and *H*−C(16)], 8.72 (br s, 2H, −CON*H*−). ^{13}C{^{1}H} NMR: δ 20.92 (−*C*H$_3$), 123.44, 125.84, 126.27, 126.71, 127.70 [quat, *C*(6)[19a] and *C*(15)], 129.64, 130.67 [quat, *C*(8) and *C*(13)], 132.40, 148.53 [quat, *C*(1) and *C*(20)], 164.95 (quat, CH$_3$O*C*O−), 169.34 [quat, *C*(7) and *C*(14). MS: *m/e* 432 [M]. R_f = 0.11 (4:1 chloroform/*n*-hexane).

1-(2-Hydroxybenzamido)-2-(2-pyridinecarboxamido)benzene (H$_3$hypyb). H$_2$hypybe (10.000 g, 26.64 mmol) was dissolved in dioxane (50 mL), and concentrated hydrochloric acid (15 mL) was added to the solution. The yellow solution was stirred overnight. Water (200 mL) was added dropwise to the stirred solution and the resulting white precipitate was filtered off and washed with water (2 × 50 mL). The product was recrystallized from toluene. Yield: 7.50 g (85%). Mp: 138 °C. Anal. Calcd for $C_{19}H_{15}N_3O_3$: C, 68.46; H, 4.54; N, 12.61. Found: C, 68.35; H, 4.60; N, 12.52. ^{1}H NMR: δ 6.91 (dd, J = 8.9, 7.4 Hz, 1H), 6.98 (d, J = 8.4, 1H), 7.22−7.31 (m, 1H), 7.32−7.45 (m, 3H), 7.48−7.55 (m, 1H), 7.77 (d, J = 8.1 Hz, 1H), 7.84−7.97 (m, 2H), 8.34 [d, J = 7.9 Hz, 1H, *H*−C(16)[19a]], 8.62 [d, J = 4.8 Hz, 1H, *H*−C(19)], 10.06 (br s, 1H), 10.27 (br s, 1H), 12.34 [s, 1H, C(1)−O*H*]. ^{13}C{^{1}H} NMR: δ 114.67 [quat, *C*(6)[19a]], 118.53, 118.89, 122.71, 124.37, 126.42 (two carbons), 126.97 (two carbons), 127.08, 129.67 [quat, *C*(8) or *C*(13)], 130.47 [quat, *C*(8) or *C*(13)], 134.38, 137.87, 148.42, 148.61 [quat, *C*15)], 162.22 [quat, *C*(1), 163.60 [quat, *C*(14)], 168.73 [quat, *C*(7)]. MS: *m/e* 333 [M]. R_f = 0.08 (4:1 chloroform/*n*-hexane).

1,2-Bis(2-hydroxybenzamido)benzene (H$_4$hybeb). The molecule was prepared by the same method as used for H$_3$hypyb above. The product was recrystallized from nitromethane (twice). Yield: 65%. Mp: 220−221 °C. Anal. Calcd for $C_{20}H_{16}N_2O_4$: C, 68.96; H, 4.63; N, 8.04. Found: C, 68.90; H, 4.62; N, 8.10. ^{1}H NMR: δ 6.95 (dd, J = 8.55, 7.6 Hz, 2H), 7.01 (d, J = 8.4 Hz, 2H), 7.22−7.31 (m, 2H), 7.47 (dd, J = 9.16, 7.3 Hz, 2H), 7.52−7.58 (m, 2H), 7.62 (d, J = 8.1 Hz, 2H), 9.00 (br s, 2H, −CON*H*−), 11.77 [s, 2H, C(1)[19a]−O*H*]. ^{13}C{^{1}H} NMR: δ 114.51[quat, *C*(6)[19a] and *C*(15)], 119.09, 119.73, 126.59, 126.76, 127.58, 130.71 [quat, *C*(8) and *C*(13)], 135.49, 162.33 [quat, C(1) and *C*(20)], 169.65 (quat, −*C*ONH). MS: *m/e* 348 [M]. R_f = 0.09 (4:1 chloroform/*n*-hexane).

***trans*-Dichloro{*N*-[2-((2-pyridylmethylene)amino)phenyl]pyridine-2-carboxamido}vanadium(III), [VCl$_2$(capca)] (1).** A solution of toluene (50 mL) containing Hcapca (0.580 g, 1.92 mmol), VCl$_3$ (0.300 g, 1.91 mmol), and triethylamine (0.400 g, 4.00 mmol) was refluxed under argon for 3 days. The resulting brown precipitate was filtered off, washed with CH$_2$Cl$_2$ (2 × 10 mL) and dried under vacuo. Yield: 0.48 g (59%). Anal. Calcd for $C_{18}H_{13}Cl_2N_4OV$: C, 51.09; H, 3.10; Cl, 16.76; N, 13.24; V, 12.04. Found: C, 51.05; H, 3.30; Cl, 16.71; N, 13.30; V, 12.15. Crystals of **1** suitable for X-ray structure analysis were obtained by slow cooling of a hot concentrated solution of the complex in acetonitrile.

{*N*-[2-((2-Phenolylmethylene)amino)phenyl]pyridine-2-carboxamido}oxovanadium(IV), [VO(phepca)] (2). H$_2$phepca (1.000 g, 3.15 mmol) was added to [VO(acac)$_2$] (0.780 g, 2.94 mmol) in methanol (40 mL). The solution was refluxed overnight during which the color of the solution changed from green to brown and a brown precipitate was formed. The solution was cooled to room temperature; the brown solid was filtered off, washed with methanol (2 × 30 mL) and diethyl ether (2 × 20 mL), and dried in vacuo to get 1.00 g (89%) of the complex. Anal. Calcd for $C_{19}H_{13}N_3O_3V$: C, 59.70; H, 3.43; N, 10.99; V, 13.32. Found: C, 59.43; H, 3.57; N, 10.84; V, 13.50. R_f = 0.05 (4:1 chloroform/*n*-hexane).

{*N*-[2-((2-Thiophenoylmethylene)amino)phenyl]pyridine-2-carboxamido}oxovanadim(IV), [VO(thipca)] (3). Hpyca (0.790 g, 3.70 mmol) and [VO(CH$_3$COO)$_2$]$_x$ (0.650 g, 3.62 mmol) were added to a stirred solution of 2-mercaptobenzaldehyde (0.500 g, 3.62 mmol) in methanol (30 mL). The solution stirred for 6 h at room temperature and then refluxed for 1 day. The resulting brown precipitate was filtered off and washed with methanol (2 × 30 mL) and diethyl ether (2 × 30 mL) and then recrystallized from CH$_3$CN and cooled to −20 °C overnigt to obtain 0.40 g (29%) of brown solid. Crystals of **3** suitable for X-ray structure analysis were obtained by slow evaporation of a dichloromethane diethyl ether (10:1) solution of the complex. Anal. Calcd for $C_{19}H_{13}N_3O_2SV$: C, 57.29; H, 3.29; N, 10.55; S, 8.05; V, 12.79. Found: C, 57.49; H, 3.33; N, 10.35; S, 8.10; V, 12.90. R_f = 0.03 (4:1 chloroform/*n*-hexane).

Sodium [1-(2-Hydroxybenzamido)-2-(2-pyridinecarboxamido)-benzenato]oxovanadate(IV), Na[VO(hypyb)].2CH$_3$OH (4·2CH$_3$OH). H$_3$hypyb (1.000 g, 3.00 mmol) was dissolved in methanol (40 mL), and solid NaOH (0.120 g, 3.00 mmol) was added under magnetic stirring. The solution was stirred until the solid NaOH was dissolved and then [VO(acac)$_2$] (0.770 g, 2.94 mmol) was added. Upon addition of the oxovanadium(IV) species, the light yellow color of the solution changed to brown*n*-green. The solution was refluxed for 4 h, after which the color of the solution changed to yellow-brown, and then the solution was concentrated to a small volume (∼5 mL). The complex was precipitated by adding dropwise, with stirring, 10 mL of diethyl ether. The brown precipitate was filtered off, washed with two 20-mL portions of diethyl ether, and dried in vacuo. Yield: 1.18 g (70%). Crystals of **4**·CH$_3$CN suitable for X-ray structure analysis were obtained by diffusion of diethyl ether into concentrated acetonitrile solution of the complex. Anal. Calcd for $C_{21}H_{20}N_3NaO_6V$: C, 52.08; H, 4.16; N, 8.68; V, 10.52. Found: C, 51.92; H, 3.98; N, 8.76; V, 10.53.

Sodium [1,2-Bis(2-hydroxybenzamido)benzenato]oxovanadate-(IV), Na$_2$[VO(hybeb)]·3CH$_3$OH (5·3CH$_3$OH). The complex was prepared in a fashion similar to that used for **4**.2CH$_3$OH except that (i) the solution was refluxed for 3 h and (ii) one more equivalent of sodium hydroxide was added. The product was obtained in 95% yield. Crystals of **5**·2CH$_3$OH suitable for X-ray structure analysis were obtained by diffusion of diethyl ether into concentrated methanol solution of the complex. Anal. Calcd for $C_{23}H_{24}N_2Na_2O_8V$: C, 49.92; H, 4.37; N, 5.06; V, 9.21. Found: C, 49.95; H, 4.32; N, 5.01; V, 9.25.

Bis[(triphenylphosphoranylidene)ammonium] [1-(2-Hydroxybenzamido)-2-(2-pyridinecarboxamido)benzenato]oxovanadate(IV), [(Ph$_3$P)$_2$N][VO(hypyb)] (6). To a stirred suspension of **4**·2CH$_3$OH (0.830 g, 1.71 mmol) in CH$_2$Cl$_2$ (30 mL) was added solid [Ph$_3$P)$_2$N]Cl (0.980 g, 1.71 mmol). After this mixture was stirred for 3 h, the complex dissolved and a white solid (NaCl) separated. After filtration and concentration of the solution to a small volume (∼5 mL), the complex was precipitated by adding dropwise, with stirring 10 mL of diethyl ether. The resulting yellow-brown precipitate was filtered off, washed with diethyl ether (2 × 15 mL), and dried in vacuo. Yield: 1.45 g (90%). Anal. Calcd for $C_{55}H_{42}N_4P_2V$: C, 70.59; H, 4.52; N, 5.99; V, 5.44. Found: C, 70.62; H, 4.60; N, 5.93; V, 5.40.

Bis[bis(triphenylphoshporanylidene)ammonium] [1,2-Bis(2-hydroxybenzamido)benzenato]oxovanadate(IV), [(Ph$_3$P)$_2$N]$_2$[VO(hybeb)] (7). The same procedure as for the above compound **6** was followed to prepare the complex, in 70% yield. Anal. Calcd for $C_{92}H_{72}N_4P_4O_5V$: C, 74.54; H, 4.88; N, 3.76; V, 3.42. Found: C, 74.30; H, 4.95; N, 3.70; V, 3.40.

Sodium [1,2-Bis(2-hydroxybenzamido)benzenato]oxovanadate-(V), Na[VO(hybeb)].CH$_3$OH (8·CH$_3$OH). Silver nitrate (0.680 g, 4.05 mmol) was added to a stirred suspension of **5**·3CH$_3$OH (2.000 g, 4.05 mmol) in CH$_3$CN (25 mL). The solution from light green immediately turned deep blue, and after a few minutes silver and sodium nitrate were precipitated. After being stirred for 3 h, the solution was filtered off and the volume of the filtrate was reduced to ∼5 mL. Diethyl ether (20 mL) was added dropwise to the stirred filtrate, and the resulting precipitate was filtered off, washed with diethyl ether, and dried in vacuo. Yield: 1.35 g (80%). Anal. Calcd for $C_{21}H_{16}N_2NaO_6V$: C, 54.09; H, 3.46; N, 6.01; V, 10.92. Found: C, 54.05; H, 3.25; N, 6.03; V, 10.90.

Bis[(triphenylphosphoranylidene)ammonium] [1,2-Bis(2-hydroxybenzamido) benzenato]oxovanadate(V), [(Ph$_3$P)$_2$N][VO(hybeb)] (9). The complex was prepared in a similar fashion to complex **6**. Yield: 65%. Anal. Calcd for $C_{56}H_{42}N_3P_2O_5V$: C, 70.81; H, 4.46; N, 4.42; V, 5.36. Found: C, 70.78; H, 4.42; N, 4.35; V, 5.40. ^{1}H NMR (l = ligand): δ 6.88 (d, J = 8.22 Hz, 2H, l), 6.98 (dd, J = 8.2, 7.5 Hz, 2H, l), 7.03 (dd, J = 5.9, 3.5 Hz, 2H, l), 7.34−7.52 (br m), 7.58−7.67 (br m), 8.12 (dd, J = 5.9, 3.5 Hz, 2H, l), 8.17 (dd, J = 7.8, 1.6 Hz, 2H, l). ^{13}C{^{1}H} NMR (l = ligand): δ 116.56 [quat, *C*(6)[19a] and *C*(15), l], 120.94 (l), 122.46 (l), 123.39 (l), 123.41 (l), 127.36 (d, J = 108 Hz, [(Ph$_3$P)$_2$N]$^+$), 129.75 (m, [(Ph$_3$)$_2$N]$^+$), 131.48 (l), 131.96 (l), 132.44 (m, [(Ph$_3$)$_2$N]$^+$), 134.02 (s, [(Ph$_3$)$_2$N]$^+$), 142.27 [quat, *C*(13) and *C*(8), l], 164.01 [quat, *C*(1) and *C*(20), l], 166.48 [quat, −*C*ON$^-$<, l].

Table 1. Crystallographic Data for the Vanadium(III) and Various Oxovanadium(IV/V) Complexes

compound	**1**·CH_3CN	**3**	**4**.CH_3CN	**5**.$2CH_3OH$	**10**
formula	$C_{20}H_{16}Cl_2N_5OV$	$C_{19}H_{13}N_3O_2SV$	$C_{21}H_{15}N_4O_4VNa$	$C_{22}H_{18}N_2O_7VNa_2$	$C_{28}H_{32}N_3O_5V$
fw	464.23	398.34	461.31	519.31	541.52
cryst. dimens, mm	0.11 × 0.16 × 0.40	0.13 × 0.20 × 0.41	0.04 × 0.06 × 0.17	0.11 × 0.28 × 0.43	0.08 × 0.10 × 0.21
a, Å	10.5991(7)	12.1108(10)	11.528(1)	12.839(1)	11.711(3)
b, Å	13.9981(7)	19.4439(18)	11.209(1)	8.334(1)	18.554(5)
c, Å	14.4021(7)	7.2351(7)	16.512(2)	12.201(1)	12.335(3)
α, deg				106.492(2)	
β, deg	98.649(2)	103.012(3)	103.928(4)	105.408(2)	95.947(9)
γ, deg				73.465(2)	
V, A^3	2112.5(3)	1660.0(4)	2071.0(5)	1175.6(3)	2666(2)
Z	4	4	4	2	4
d_{calcd}/d_{measd} (g cm^{-3})	1.460/1.45	1.594/1/57	1.480/1.47	1.467/1.45	1.350/1.33
space group	$P2_1/n$	$P2_1/n$	$P2_1/c$	$P1$	$P2_1/c$
temp, K	296	298	296	296	296
radiation; λ, Å	Mo Kα; 0.7107	Mo Kα; 0.7107	Mo Kα; 0.7107	Mo Kα; 0.7107	Mo Kα; 0.7107
abs coeff (*ρ*), cm^{-1}	7.70	7.29	5.50	4.80	4.00
max. abs. cor factor	1.08	1.08	1.14	1.23	
no. of data collcd/unique	4547/4138	3753/3258	2377/2135	4261/4047	2562/2306
no. of data used	3063 [$F_o > 5.0\sigma(F_o)$]	2367 [$F_o > 4.0\sigma F_o$)]	1774 [$F_o > 3.0\ \sigma(F_o)$]	3102[$F_o > 7.0\ \sigma(F_o)$]	1839[$F_o > 2.0\ \sigma(F^\circ)$]
$R = \sum\|\|F_o\| - \|F_o\|\|/\sum\|F_o\|$	0.0323	0.0355	0.0649	0.0894	0.0904
$R_w = [\sum w\{\|F_o\| - \|F_o\|\}^2 \sum w\|F_o\|^2]^{1/2}$	0.0335	0.0376	0.0806[a]	0.1043	0.0879

[a] $w = 1/\sigma^2(F_o) + 0.0006F_o^2$.

Tetraethylammonium [1,2-Bis(2-hydroxybenzamido)benzenato]-oxovanadate(V), Et_4N[VO(hybeb)].CH_2Cl_2 (10·CH_2Cl_2). The complex was prepared in a fashion similar to that used for complex **6** except Et_4NCl was used instead of $(Ph_3P)_2NCl$ to get the complex in 67% yield. Anal. Calcd for $C_{29}H_{34}Cl_2N_3O_5V$: C, 55.60; H, 5.47; N, 6.71; V, 8.13. Found: C, 55.60; H, 5.36; N, 6.73; V, 8.10. Crystals of Et_4N[VO(hybeb)] suitable for X-ray structure analysis were obtained by diffusion of diethyl ether into concentrated nitromethane solution of the complex.

X-ray Crystallography. Diffraction measurements were made on a $P2_1$, Nicolet diffractometer upgraded by Crystal Logic using Zr-filtered Mo-radiation. Unit cell dimensions were determined and refined by using the angular settings of 25 automatically centered reflections in the range $11 < 2\theta < 24°$, and they appear in Table 1. All crystals used for data collection were mounted on glass fibers and coated with epoxy glue. Crystals of the complexes **1**·CH_3CN, and **3** were of good quality and sufficient size; crystals of complex **5**·$2CH_3OH$ were of good size but poor quality (polycrystalites on the surface), and crystals of the complexes **4**·CH_3CN and **10** were very small and of poor quality. Intensity data were recorded using a $\theta-2\theta$ scan with scan speed 4.5 deg/min (**1**·CH_3CN, **5**·$2CH_3OH$, **3**) or 1.5 deg/min (**4**·CH_3CN, **10**) and scan range 2.4° (**1**·CH_3CN), 2.5° (**3**, **5**·$2CH_3OH$, **10**), 2.9° (**4**·CH_3CN) plus $\alpha_1\alpha_2$ separation. Three standard reflections monitored every 97 reflections showed less than 3% variation but **5**·$2CH_3OH$ displayed a 21% decay which was corrected. Lorentz, polarization and *ψ*-scan absorption (except for **10**) corrections were applied using Crystal Logic software. All structures were solved by direct methods using SHELXS-86[20] and refined by full-matrix least-squares techniques with SHELX-76,[21] using unit weights (except for **4**·CH_3CN).

Complex 1 ·CH_3CN. Data were collected in the range $0 < h < 13$, $0 < k < 17$, $-17 < l < +17$ ($2\theta_{max} = 52°$). Symmetry equivalent data were averaged with $R = 0.0252$ to give 4138 unique reflections from a total 4547 collected. All hydrogen atoms (except those of a methyl group) were located by difference maps and their positions were refined isotropically. All non-hydrogen atoms were refined anisotropically. The final values for *R* and R_w for observed data are given in Table 1, for all data they are 0.0508 and 0.0467, respectively. The maximum and minimum residual peaks in the final difference map were +0.337 and −0.257 e/$Å^3$. The largest shift/esd in the final cycle was 0.053.

Complex 3. Data were collected in the range $-14 < h < +14$, $0 < k < 23$, $-8 < l < 0$ ($2\theta_{max} = 52°$). Symmetry equivalent data were averaged with $R = 0.0254$ to give 3258 unique reflections from a total of 3753 collected. All hydrogen atoms were located from difference Fourier maps and their positions were refined isotropically. All non-hydrogen atoms were refined anisotropically. The final values of *R* and R_w for observed data are given in Table 1; for all data they are 0.0601 and 0.0587, respectively. The maximum and minimum residual peaks in the final difference map were +0.309 and −0.285 e/$Å^3$. The largest shift/esd in the final cycle was 0.002.

Complex 4·CH_3CN. Data were collected in the range $-11 < h < 11$, $0 < k < 11$, $0 < l < -16$ ($2\theta_{max} = 41.6°$). Symmetry equivalent data were averaged with $R = 0.0283$ to give 2135 independent reflections from a total of 2377 collected; hydrogen atoms were introduced at ideal positions as riding on bonded atoms at 0.96 Å. All non-hydrogen atoms were refined anisotropically. The final values for *R*, R_w for observed given data are in Table 1; for all data they are 0.0783 and 0.0828, respectively. The maximum and minimum residual peaks in the final difference map were +1.081 and −0.542 e/$Å^3$. The largest shift/esd in the final cycle was 0.002.

Complex 5·$2CH_3OH$. Data were collected in the range $0 < h < 11$, $-9 < k < +10$, $-15 < l < +14$ ($2\theta_{max} = 52°$). Symmetry equivalent data were averaged with $R = 0.0261$ to give 4047 independent reflections from a total of 4261 collected. Only the hydrogen atoms of the phenyl groups were located by difference maps, and their positions were refined isotropically. The rest were introduced at ideal positions as riding on bonded atoms at 0.96 Å. All non-hydrogen atoms were refined anisotropically. The final values for *R* and R_w for observed data are given in Table 1; for all data they are 0.1192 and 0.1381, respectively. The maximum and minimum residual peaks in the final difference map were +2.176 and −0.900 e/$Å^3$. The largest shift/esd in the final cycle was 0.025.

Complex 10. Data were collected in the range $-10 < h < +10$, $0 < k < 17$, $0 < l < 11$ ($2\theta_{max} = 39$). Symmetry equivalent data were averaged with $R = 0.0401$ to give 2306 unique reflections from a total of 2562 collected. All hydrogen atoms were introduced at ideal positions as riding on bonded atoms at 0.96 A. All non-hydrogen atoms were refined anisotropically. The final values for *R* and R_w for observed data are given in Table 1, for all data they are 0.1244 and 0.1123, respectively. The maximum and minimum residual peaks in the final difference map were +0.464 and −0.381 e/$Å^3$. The largest shift/esd in the final cycle was 0.046.

Physical Measurements. Infrared spectra of the various compounds dispersed in KBr pellets were recorded on a Perkin-Elmer 577 spectrometer. A polystyrene film was used to callibrate the frequency. Electronic absorption spectra were measured as solutions in septum-sealed quartz cuvettes on a Perkin-Elmer Lambda 15 UV/vis spectrophotometer. Electron impact mass spectral data were obtained with a

(20) Sheldrick, G. M. SHELXS-86: Structure Solving Program, University of Gottingen, Germany, 1986.
(21) Sheldrick, G. M. SHELX-76: Program for Crystal Structure Determination, University of Cambridge, England, 1976.

Kratos MS25RFA spectrometer. Melting points were determined (uncorrected) with a Buchi melting point apparatus. Magnetic moments were measured at room temperature by the Faraday method, with mercuric tetrathiocyanatocobaltate(II) as the susceptibility standard on a Cah*n*-Ventron RM-2 balance. The EPR were recoreded on a Bruker EPR 300 spectrometer. The spectrometer was operating at X-band (9.449 GHz) with a microware power of 200 μW, a modulation frequency of 100 KHz, a modulation amplitude of 7.95 G, a time constant of 20.48 ms, a conversion time of 81.92 ms, a central field of 3400 G and a sweep width of 2000 G. Diphenylpicrylhydrazyl, g = 2.0037, was used for calibration. A Bruker (VT-100) flow-through variable temperature controller provided temperatures of 120−140 K at the sample position in the cavity.

NMR Studies. The NMR experiments of this study were performed on a Bruker AC-300 NMR spectrometer (7.0 T) equipped with a 5 mm probe for ^{1}H and ^{13}C spectra and with a 10 mm broad-band probe for the ^{51}V spectrum. All spectra were recorded at 300 K. Compounds Hcapca, H_2phepca, H_2hypybe, H_3hypyb, and H_2hybebe were dissolved in $CDCl_3$ (spectroscopic grade, 99%+) while compounds H_4hybeb and complex **9** were dissolved in CD_2Cl_2 (spectroscopic grade, 99%+). The following solutions were prepared: Hcapca, 32 mg/0.5 mL, H_2phepca, 6 mg/0.5 mL: H_2hypybe, 33 mg/0.5 mL; H_3hypyb, 7 mg/0.5 mL; H_2-hybebe, 31 mg/0.5 mL; H_4hybeb, 2 mg/0.5 mL; **9**; 30 mg/0.5 mL dry CD_2Cl_2 and 10 mg/2.0 mL dry CD_2Cl_2 for the 10 mm probe. TMS was added in the tubes as ^{1}H and ^{13}C chemical shift reference.

^{1}H and ^{13}C spectra were acquired using standard parameters. More particularly, ^{13}C spectra were acquired with a spectral window of 220 ppm, a 90° pulse, a relaxation delay of 2 s, and under proton decoupling. A 2.4 Hz exponential broadening was applied to the FID prior to the Fourier transformation.

The ^{51}V spectrum of the complex was acquired at 78.899 MHz with a spectral width of 1060 ppm, a 90° pulse, and a relaxation delay of 0.5 s. A 20 Hz line broadening factor was applied before the Fourier transformation. The chemical shifts are reported with respect to $VOCl_3$ at 0 ppm as external reference.

Electrochemistry. Electrochemical experiments were performed with a Metrohm E629 Polarecord-VA-Scanner E612 apparatus connected to a Houston 2000 XY recorder. Platinum disk and dropping mercury electrodes (DME) were employed as working electrodes for the cyclic voltammetric and polarographic studies, respectively. A platinum wire was used as an auxiliary electrode, while a silver/silver chloride electrode in dichloromethane (saturated with tetrabutylammonium tetrafluoroborate) or acetonitrile (saturated with tetraethylammonium perchlorate) was used as a reference electrode. The supporting electrolytes in dichloromethane and acetonitrile were tetrabutylammonium tetrafluoroborate and tetraethylammonium perchlorate (0.1 M) respectively, and all solutions were 10^{-3}−10^{-4} M in complex. Values for the reduction potential ($E_{1/2}$) and the number of electrons involved in the reversible process were obtained from the intercept and the slope of the plot of $\ln[(i_d - i)/i]$ vs potential (E) according to the Heyrovsky−Ilkovic equation[22]

$$E = E_{1/2} + (RT/nF)(\ln[(i_d - i)/i]) \quad (1)$$

All potentials throughout this paper are relative to the normal hydrogen electrode (NHE)[23] using ferrocene (+0.400 V vs NHE)[24] as a standard.

Results and Discussion

Syntheses. The ligands used in this study are shown in Chart 1. The ligands Hcapca and H_2phepca were prepared by condensing Hpyca with either 2-pyridinecarboxaldehyde or salicylaldehyde in methanol respectively, while the ligand H_3hypyb was synthesized by the route depicted in Scheme 1. The organic molecule H_4hybeb was prepared in a fashion similar to that used for H_3hypyb, which is different from the literature-reported method for its synthesis.[25] The synthesis of all of the ligands was followed by thin-layer chromatography.

Complex **1** was prepared by reacting vanadium(III) chloride with Hcapca and triethylamine (eq 2) in refluxing toluene for 3

Chart 1. Ligands Used in This Study[a]

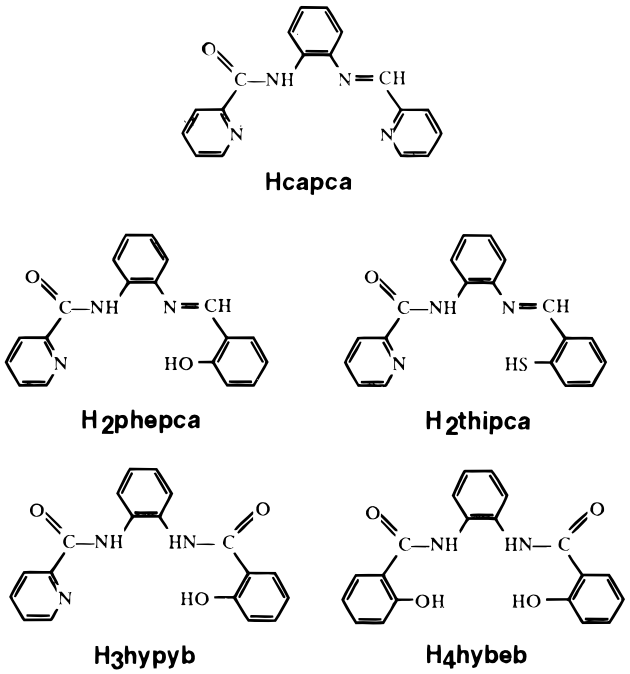

Scheme 1. Synthesis of the Ligand H_3hypyb[a]

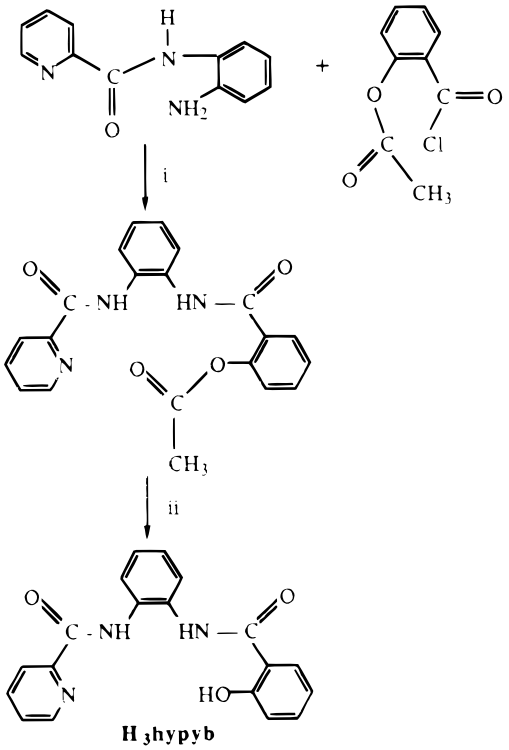

[a] Reagents and conditions: i, dioxane, argon; ii, dioxane, aqueous concentrated hydrochloric acid.

(22) Heyrovsky, I.; Ilkovic, D. *Collect. Czech. Chem. Commun.* **1935**, 7, 198.
(23) Gagne, R. R.; Koval, C. A.; Lisensky, G. C. *Inorg. Chem.* **1980**, 19, 2854.
(24) Koepp, H. M.; Wendt, H.; Strehlow, H. *Z. Elektrochem.* **1960**, 64, 483.
(25) Anson, F. C.; Collins, T. J.; Gipson, S. L.; Keech, J. T.; Krafft, T. E.; Peake, G. T. *J. Am. Chem. Soc.* **1986**, 108, 6593.
(26) Addison, A. W.; Rao, T. N.; Reedijk, J.; Rijn, J.; Verschoor, G. C. *J. Chem. Soc., Dalton Trans* **1984**, 1349.

$$VCl_3 + Hcapca + Et_3N \rightarrow \mathbf{1} + Et_3NHCl \quad (2)$$

days. When nitromethane, acetonitrile, or methanol were used as solvents, we failed to isolate the V^{III} complex and oxo species were isolated instead.

Complex **3** was synthesized via a template condensation reaction of Hpyca with 2-mercaptobenzaldehyde in the presence of $[VO(CH_3COO)_2]_x$ (eq 3). When $[VO(acac)_2]$ was used

$$Hmeba + Hpyca + [VO(CH_3COO)_2]_x \rightarrow \mathbf{3} + 2CH_3COOH \quad (3)$$

instead of $[VO(CH_3COO)_2]_x$, the product was contaminated by $[VO(pycac)]$[7b] which presumably resulted from condensation of Hpyca with the coordinated $acac^-$.

The method of ligand substitution was employed for the preparation of the $V^{IV}O^{2+}$ complexes (except of course for complex **3**) in refluxing methanol. In addition sodium hydroxide was used as a base for the synthesis of the anionic complexes **4**·$2CH_3OH$ and **5**·$3CH_3OH$ (eq 4).

$$[VO(acac)_2] + H_4hybeb + 2NaOH \rightarrow \mathbf{5} + 2Hacac + 2H_2O \quad (4)$$

Oxidation of the compound **5**·$3CH_3OH$ is readily accomplished using silver nitrate in acetonitrile (eq 5) or any other silver salts,

$$\mathbf{5} + AgNO_3 \rightarrow \mathbf{8} + NaNO_3 + Ag \quad (5)$$

with the soluble product being readily separated from $NaNO_3$ and silver. Efforts to prepare the complex $[V^{V}O(hypyb)]$ have so far proven unsuccessful. The sodium salts of the complexes **4**·$2CH_3OH$, **5**·$3CH_3OH$, and **8**·CH_3OH are readily converted to the corresponding $[(Ph_3P)_2N]^+$ salts by reacting them with $[Ph_3P)_2N]Cl$ in dichloromethane.

When complexes **4**·$2CH_3OH$ and **5**·$3CH_3OH$ are dissolved in water in the presence of air, they are hydrolyzed−oxidized to their corresponding ligands and different vanadium(V) species as is evidenced from ^1H, $^{13}C\{^1H\}$, and ^{51}V NMR studies of the decomposition products. Addition of water into an acetonitrile solution of **8**·CH_3OH in air results in dissociation of its ligand. The sodium salts of the anionic complexes (**4**, **5**, and **8**) and the tetraethylamonium salt of the vanadium(V) complex are air sensitive in solution and in the solid state as well. They gradually lose their solubility even under inert atmosphere with time. In marked contrast their corresponding $[(Ph_3P)_2N]^+$ salts are reasonably stable in air in both solution and the solid state and are indefinitely stable under inert atmosphere as solids. The solubility of complex **1** is reduced with time.

X-ray Crystal Structures. The structure of the complex **1**·CH_3CN as illustrated in Figure 1, showed the vanadium atom possessing a distorted octahedral coordination with the N_4 set of atoms from the $capca^-$ ligand in the equatorial plane and the chlorine atoms in the axial positions. The four N-donor atoms define an almost perfect plane, with the largest out of plane displacement of 0.015 Å (Table 4) by N(3). Of the four V−N bonds, the bond to N(3), the deprotonated amide nitrogen, constitutes the shortest V−N distance [1.982(2) Å] so far reported for octahedral vanadium(III) complexes. This is in agreement with the fact that the deprotonated amide nitrogen is a very strong σ-donor. It is worth noting that the vanadium-deprotonated amide nitrogen bond distance [mean $V-N_{amide}$ = 1.999(12) Å, from Table 5] does not vary significantly with oxidation state of vanadium(III, IV, and V), geometry (octahedral vs square pyramidal), and charge−donor set of the complexed ligand, −1 (N_4), −2 (N_3O,N_3S), −3 (N_3O), or −4 (N_2O_2), as is obvious from Table 5. The amide group is planar within the limits of precision (Table 4). The bond lengths to N(1) [2.175(2) Å] and N(4) [2.124(2) Å], the pyridine nitrogens, are substantially longer than the V−N(3) bond distance and are different from each other as a consequence of the difference in the *trans* atoms [N(3) and N(2), respectively]. The bond length to N(2) [2.058(2) Å], the imine nitrogen, is close to those found in the vanadium(III)−Schiff base complexes.[27] The V−Cl bond lengths [V−Cl(1) 2.340(1) and V−Cl(2) 2.313(1) Å] (Table 3)

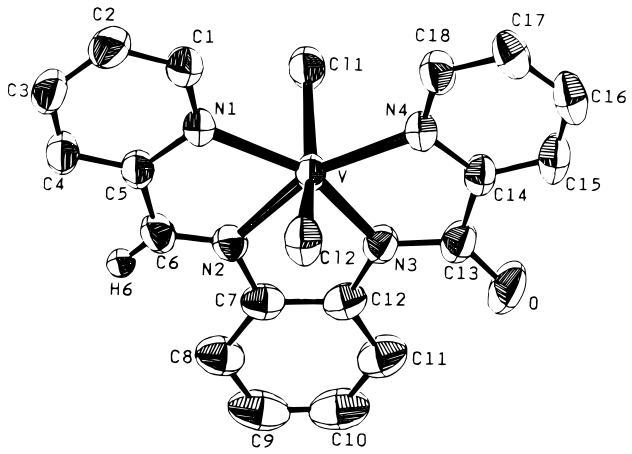

Figure 1. Molecular structure of **1**·CH_3CN with the atoms represented by their 50% probability ellipsoids for thermal motion.

Table 2. Interatomic Distances (Å) and Angles (deg) Relevant to the Vanadium(IV/V) Coordination Sphere

parameter	**3**	**4**·CH_3CN	**5**.$2CH_3OH$	**10**
V−O(1)	1.590(2)	1.595(4)	1.609(6)	1.579(8)
V−O(2)		1.887(4)	1.918(6)	1.829(8)
V−O(5)			1.917(7)	1.783(8)
V−N(1)	2.077(3)	2.016(5)	2.037(8)	1.977(8)
V−N(2)	1.997(3)	2.001(5)	2.007(7)	2.008(8)
V−N(3)	2.106(3)	2.107(5)		
V−S	2.322(1)			
O(1)−V−O(2)		110.9(2)	113.3(3)	106.2(4)
O(1)−V−N(1)	104.0(1)	106.9(2)	104.1(3)	102.7(4)
O(2)−V−N(1)		91.8(2)	87.6(3)	86.5(3)
O(1)−V−N(2)	112.2(1)	112.1(2)	108.5(3)	101.6(4)
O(2)−V−N(2)		136.8(2)	138.1(3)	150.9(4)
N(1)−V−N(2)	78.4(1)	79.5(2)	79.7(3)	78.9(3)
O(1)−V−N(3)	104.5(1)	105.8(2)		
O(1)−V−O(5)			102.0(3)	106.9(5)
O(2)−V−N(3)		88.1(2)		
O(2)−V−O(5)			85.5(3)	94.5(4)
N(1)−V−N(3)	148.0(1)	145.0(2)		
N(1)−V−O(5)			153.7(3)	148.8(5)
N(2)−V−N(3)	77.7(1)	76.9(2)		
N(2)−V−O(5)			88.6(3)	85.7(4)
S−V−O(1)	111.6(1)			
S−V−N(1)	91.7(1)			
S−V−N(2)	136.2(1)			
S−V−N(3)	90.9(1)			

Table 3. Interatomic Distances (Å) and Angles (deg) Relevant to the Vanadium(III) Coordination Sphere for **1**·CH_3CN

V−Cl(1)	2.340(1)	V-N(2)	2.058(2)
V−Cl(2)	2.313(1)	V-N(3)	1.982(2)
V−N(1)	2.175(2)	V-N(4)	2.124(2)
Cl(1)−V−Cl(2)	159.8(1)	N(1)-V-N(3)	155.3(1)
Cl(1)−V−N(1)	83.8(1)	N(2)-V-N(3)	79.4(1)
Cl(2)−V−N(1)	83.0(1)	Cl(1)-V-N(4)	88.4(1)
Cl(1)−V−N(2)	97.5(1)	Cl(2)-V-N(4)	87.1(1)
Cl(2)−V−N(2)	93.9(1)	N(1)-V-N(4)	125.6(1)
N(1)−V−N(2)	75.9(1)	N(2)-V-N(4)	158.3(1)
Cl(1)−V−N(3)	100.1(1)	N(3)-V-N(4)	79.0(1)
Cl(2)−V−N(3)	98.3(1)		

Table 4. Comparison of a Few Characteristic Crystallographic Data for Vanadium(III, IV, and V) Complexes with Amidate Ligands

complex	**1**·CH_3CN	**3**	**4**·CH_3CN	**5**·$2CH_3OH$	$[V^{IV}O(depa\text{-}H)]^{2-}$	**10**	$[V^{V}O(hymeb)]^{-}$
largest deviation from the mean plane,[a] Å	0.015	0.260	0.086	0.180	0.027[b]	0.011	0.240
vanadium displacement from the mean plane,[a] Å	0.071	0.642	0.642	0.589	0.609[b]	0.473	0.440
amide planarity,[c] deg	1.7	6.1	2.7, 2.8[d]	4.9, 6.9[d]	8.7,[b] 18.7[b,d]	0.8, 3.5[d]	3.5, 6.5[d]
trigonality index[e] (τ)		0.197	0.140	0.26	0.06[b]	0.04	0.08
ref	this work	this work	this work	this work	9	this work	10

[a] The mean plane is defined by the four atoms of the tetradentate ligands. [b] These values represenent an average of the two values for the two independent molecules in the asymmetric unit. [c] The amide planarity is defined by the four atoms O−C−N−C around the C−N bond; which is zero for perfect planarity. [d] These ligands are diamidic. [e] The trigonality index,[26] τ, is given by the equation, $\tau = (\varphi_1 - \varphi_2/60)$, where φ_1 is the largest angle and φ_2 is the next largest angle in the coordination sphere ($\tau = 0/1$ for square pyramidal/trigonal bipyramidal geometries, respectively).

Table 5. Correlation between $V-N_{amide}$ Bond Distances,[a] Oxidation States Geometries,[b] and Charge−Donor Set of the Complexed Ligand

complex	$V-N_{amide}$, Å	charge, donor set of the complexed ligand	ref
$[V^{III}Cl_2(capca)]$[b] (**1**·CH_3CN)	1.982(2)	−1, N_4	this work
$[V^{IV}O(pycac)]$	1.979(5)[c]	−2, N_3O	7b
$[V^{IV}O(pycbac)]$	1.989(2)	−2, N_3O	7b
$[V^{IV}O(thipca)]$ (**3**)	1.997(3)	−2, N_3S	this work
$[V^{IV}O(hypyb)]^{-}$ (**4**$^{-}$·CH_3CN)	2.009(8)	−3, N_3O	this work
$[V^{IV}O(hybeb)]^{2-}$ (**5**$^{2-}$·$2CH_3OH$)	2.022(15)[d]	−4, N_2O_2	this work
$[V^{IV}O(depa-H)]^{2-}$	2.013(1)[c,d]	−4, N_2O_2	9
$[V^{V}O(hybeb)]^{-}$ (**10**$^{-}$)	1.993(15)[d]	−4, N_2O_2	this work
$[V^{V}O(hymeb)]^{-}$	2.007(2)[d]	−4, N_2O_2	10
mean	1.999(12)		

[a] The vanadium(II)[8]−N_{amide} bond length has not been included in this table because the amide functionality (−CON^{-}−) in this case acts as a bridging three-center chelating ligand and as a bridging−chelating ligand as well through oxygen and deprotonated amide nitrogen, and so this mode of coordination precludes direct comparison with the other $V-N_{amide}$ bond distances reported in this table, where the −CON^{-}− functionality is coordinated only through the deprotonated amide nitrogen to vanadium. [b] Only the vanadium(III) complex has an octahedral geometry; all other complexes in this table have a square pyramidal geometry. [c] Mean value of the four $V-N_{amide}$ bonds. [d] This bond distance represents the mean value of two $V-N_{amide}$ bonds for each complex.

are slightly shorter than those reported for other V(III)−Schiff base complexes[28] and different from each other as a result of a hydrogen bond between H(6) and Cl(1) [C(6)−H(6) = 0.91(3) Å, H(6)···Cl(1) = 2.85(3) Å, and C(6)−H(6)···Cl(1) = 153-(2)°].

Figure 2 shows a perspective view of **3**. The vanadium is in a distorted square pyramidal environment consisting of a pyridine nitrogen, a deprotonated amide nitrogen, an imine nitrogen, and a thiophenolate sulfur in the basal plane (that is a {S,N} system and the first N_3S system for the VO^{2+} center) and an oxo ligand occupying the apical position. The vanadium atom is 0.642 Å (Table 4) above the mean plane defined by the basal atoms. The trigonal distortion of the square pyramid (τ = 0.197, Table 4) is primarily due to the presence of the large sulfur atom in the basal plane. The $V-N_{amide}$ bond distance of 1.997(3) Å is indicative of a strong bond of the deprotonated amide nitrogen to vanadium. The V−S bond length is 2.322-(1) Å. A comparison of the V−S bond length, with the V−S bond distances, of the only two other structural studies of square

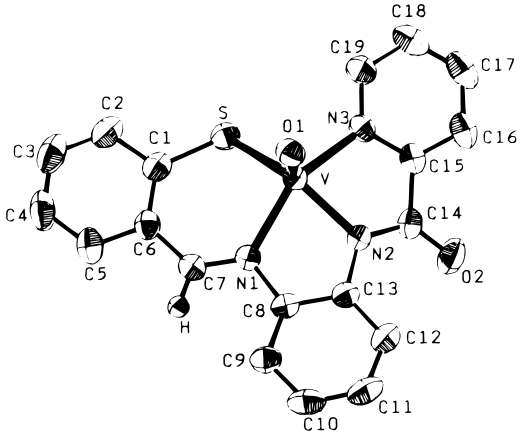

Figure 2. ORTEP drawing of the molecular structure of **3** showing the atom-labeling scheme. Atoms are represented by their 50% probability ellipsoids.

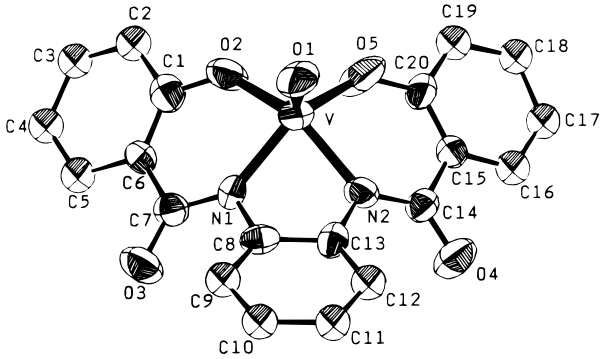

Figure 3. ORTEP drawing of the anion **10**$^{-}$ at 50% probability ellipsoids giving atomic numbering.

pyramidal geometry, with {S,N} chelates of oxovanadium(IV), which were made on bis(L-cysteinato methyl ester-*N*,*S*)oxovanadium(IV)[29] [2.322(3) Å] and on [*N*,*N*′-ethylenebis(thiosalicylideneaminato)]oxovanadium(IV)[30] [(V−S) = 2.346 Å] complexes, reveals that the V−S distances in all these complexes are almost the same.

The molecular structure of the complex anion **10**$^{-}$, the vanadium(V) complex, is shown in Figure 3. The complex anion adopts a square pyramidal geometry (spg) with almost no trigonal distortion (τ = 0.04, Table 4) while its vanadium-(IV) analogue (Figure 4) deviates substantially from the spg (τ = 0.26, Table 4). The V^{V}═O bond length at 1.579(8) Å, is 0.03 Å shorter than the V^{IV}═O bond length (Table 2). The "hard" $V^{V}O^{3+}$ ion shows a strong preference for phenolate coordination when compared to the "softer" $V^{IV}O^{2+}$ ion, which is reflected in the $V-O_{phenolate}$ bond distance [average V−O 1.81 and 1.92 Å for vanadium(V) and vanadium(IV) respec-

(27) Hosset, J. M.; Floriani, C.; Mazzanti, M.; Chiesi-Villa, A.; Guastini, C. *Inorg. Chem.* **1990**, 29, 3991.
(28) (a) Mazzanti, M.; Floriani, C.; Chiesi-Villa, A.; Guastini, C. *Inorg. Chem.* **1986**, 25, 4158. (b) Mazzanti, M.; Gambarotta, S.; Floriani, C.; Chiesi-Villa, A.; Guastini, C. *Inorg. Chem.* **1986**, 25, 2308.
(29) Sakurai, H.; Jaira, Z.; Sakai, N. *Inorg. Chim. Acta* **1988**, 151, 85.
(30) Dutton, J. C.; Fallon,G. D.; Murray, K. S. *Inorg. Chem.* **1988**, 27, 34.

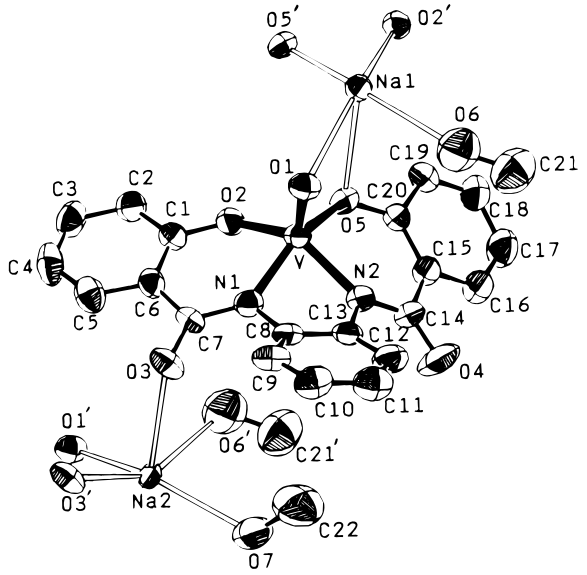

Figure 4. ORTEP drawing of **5**·2CH_3OH at 50% probability ellipsoids giving atomic numbering and the interactions of the sodium atoms with various oxygen atoms.

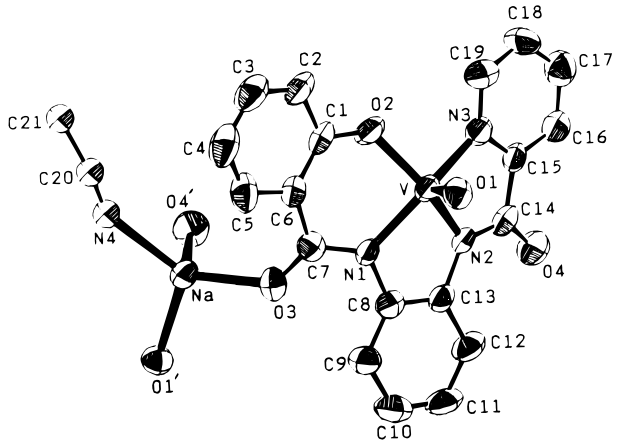

Figure 5. ORTEP drawing of **4**·CH_3CN at 50% probability ellipsoids giving atomic numbering and coordination environment of the sodium atom.

tively]. These $V^{IV/V}-O_{phenolate}$ bond lengths are almost identical with the literature[31] reported values for the pair of complexes, $[V^{V}O(salen)]ClO_4$[31a] (**1′**) and $[V^{IV}O(salen)]$[31b] (**2′**), being 1.80 and 1.92 Å for **1′** and **2′**, respectively. On the other hand, there are no significant differences in the $V-N_{amide}$ bond lengths (average V−N 2.02 and 1.99 Å for vanadium(IV) and vanadium(V) respectively). The sodium ions interact very weakly with various oxygen atoms (Figure 4). The shortest contacts are Na(1)−O(2) = 2.734(7) Å and Na(2)−O(7) = 2.695(9) Å for Na(1) and Na(2) respectively.

The crystal structure of the complex **4**·CH_3CN (Figure 5) does not differ appreciably from the X-ray structures of the oxovanadium(IV/V) complexes discussed above. Two only points merit a comment. The first is that the bond to O(2), the phenolate oxygen, constitutes the shortest V−O distance [1.887(4) Å] so far reported for oxovanadium(IV) species. The second is that the sodium atom lies in a distorted tetrahedral environment with three strong bonds to oxygen atoms, {two amide ones [Na−O(4) = 2.230(5) and Na−O(3) = 2.242(5) Å] from two different anionic vanadium(IV) complex anions, and an oxo group [Na−O(1) = 2.3111(5) Å]} and a weaker bond to the nitrogen atom of the acetonitrile solvent [Na−N(4) = 2.444(9) Å]. The six angles of the tetrahedron vary between 91.4(2) and 129.6(3)°.

Table 6. EPR Parameters

					A, $cm^{-1} \times 10^{-4}$		
compound	donor set	$g_{\|\|}$	$g_\perp$	g_0	$A_{\|\|}$	$A_\perp$	A_0
2	N_3O	1.957	1.975	1.969	152.4	54.8	87.3
3	N_3S	1.965	1.980	1.975	150.6	52.3	85.0
6	N_3O	1.960	1.976	1.970	156.1	52.2	86.8
7	N_2O_2	1.960	1.978	1.972	156.2	53.6	87.8

Magnetism and Electron Paramagnetic Spectra. The complexes **2**, **3**, **6**, and **7** have magnetic moments of 1.78, 1.76, 1.75, and 1.76 μ_B respectively in accord with spin-only value of a d^1 system, whereas the vanadium(V) complex, **9**, which is a d^0 system, is diamagnetic. The complex **1** has a magnetic moment of 2.71 μ_B as expected for a d^2 system.

The isotropic (liquid solution) EPR spectra of the oxovanadium(IV) complexes, namely **2**, **3**, **6**, and **7**, reveal eight resonances attributable to a single $S = {}^1/_2$ species in which the unpaired electron in a d_{xy} orbital is coupled to the nuclear spin of the vanadium nucleus (^{51}V, 99.76 atom %, $I = {}^7/_2$, $\mu = 5.149$ B_N). These results are consistent with the magnetic moments and show that ligand dissociation has not occured during the preparation of the EPR samples.

The EPR parameters (from anisotropic spectra) for the oxovanadium(IV) complexes (Table 6) were determined by computer simulation of the experimental EPR spectrum. As it is obvious from the data of Table 6, only subtle changes are observed between the parameters of these complexes, despite the different equatorial ligand field strengths for N_2O_2, N_3O, and N_3S. However, qualitatively, data of the type given in Table 6 should prove useful for identifying donor atoms bound to VO^{2+} unit in proteins and enzymes.

NMR Studies. Characteristic ^1H NMR and proton-decoupled ^{13}C NMR resonances and their attribution for the organic molecules Hcapca, H_2phepca, H_2hypybe, H_3hypyb, H_2hybebe, and H_4hybeb are summarized in the experimental section. The attribution of the resonances was based on the literature[32] and comparisons between molecules of this study.

^{51}V Spectrum of 9. The spectrum shows one resonance signal at −465 ppm (referred to $VOCl_3$) with half-height line width $\Delta\nu_{1/2}$ of 122 Hz ($1/\Delta\nu_{1/2} = 8.2$ ms), after subtraction of the 20 Hz line broadening introduced during the processing. This peak appears at a chemical shift similar to that of the closely related complex potassium [1,2-bis(2-hydroxy-2-methylpropanamido)benzenato]oxovanadate(V),[10] which was recently reported to have a ^{51}V resonance peak at −455 ppm.

The chemical shift and line width for complex **9**, which is an {N,O} system, are in agreement with an already published empirical correlation[33] between these two parameters, showing that relatively high $1/\Delta\nu_{1/2}$ values (5−8 in ms) combined with relatively high ^{51}V chemical shifts (-480 to −490 ppm) are characteristic of an {N,O} pentacoordinated vanadium(V) species.[33]

^{1}H and ^{13}C Spectra of the Free Ligand, H_4hybeb, and of Its Corresponding Vanadium(V) Complex. The comparison between the proton NMR spectrum of the free ligand H_4hybeb and the proton spectrum of the vanadium(V) complex **9** showed three main effects due to the complexation.

(31) (a) Bonadies, J. A.; Butler, W. M.; Pecoraro, V. L.; Carrano, C. J. *Inorg. Chem.* **1987**, 26, 1218. (b) Riley, P. E.; Pecoraro, V. L.; Carrano, C. J.; Bonadies, J. A. *Inorg. Chem.* **1987**, 25, 154.

(32) Pretsch, E.; Seibl, J.; Simon, W.; Clerc, T. *Spectral Data for Structure Determination of Organic Compounds*, English translation of the revised 2nd German Ed.; Springer-Verlag: Berlin, Heidelberg, Germany, 1983.

(33) Crans, D. C.; Shin, P. K. *J. Am. Chem. Soc.* **1994**, 116, 1305.

Table 7. Quaternary Carbon Resonances of the Vanadium(V) Complex and of the Free Ligand.

	Ph[a]−CO−	*Ph*[a]−N<	*Ph*[a]−O−	Ph−*C*ON<
H_4hybeb	114.51	130.71	162.33	169.65
9	116.56	142.27	164.01	166.48
$\Delta\delta = \delta_{comp} - \delta_{free}$	2.05	11.56	1.68	−3.17

[a] ^{13}C resonance of the ring carbon attached to substituent shown.

(i) The first effect was the absence of the amidic (δ = 9.00 ppm) and phenolic (δ = 11.77 ppm) proton signals from the complex's spectrum, as expected due to the V^V−N and V^V−O bond formation.

(ii) The second effect was the expansion toward downfield chemical shifts of the aromatic proton signals range. These signals in the free ligand's spectrum are located between 6.93 and 7.60 ppm ($\Delta\delta$ = 0.67 ppm), while in the complex's spectrum they lie between 6.85 and 8.15 ppm ($\Delta\delta$ = 1.30 ppm). This downfield effect has also been observed in other vanadium-(V) complexes.[34]

(iii) The third effect was the appearnce of the $[(Ph_3P)_2N]^+$ peaks (broad multiplets δ = 7.25−7.53 and 7.53−7.65 ppm) which overlaps one of the ligand's peaks.

The ^{13}C spectrum of the free ligand contains 10 signals corresponding to the 20 carbons of the molecule owing to its symmetry. Among these 10 carbon resonances, four signals are belonging to quaternary carbons and can be easily distinguished and attributed by using the standard literature values[32] as follows: δ = 114.51, *Ph*[19b]−CO−; 130.71, *Ph*[19b]−NH−; 162.33, *Ph*[19b]−OH and 169.65, Ph−*C*ONH−.

In contrast, the ^{13}C spectrum of the complex **9** is more complicated due to the superposition of the ligand's signals with those of the cation $[(Ph_3P)_2N]^+$. The *Ph*[19b]−O− and Ph−*C*ON< peaks of complex **9** can not be observed under standard acquisition conditions due to their very long T_1s. They have been detected at 164.01 and 166.48 ppm only by using the inverse gate sequence with a relaxation delay of 300 s.

In Table 7 are shown the characteristic quaternary carbon resonances of the vanadium(V) complex (**9**) and of the free ligand together with the coordination-induced shift (CIS) values defined as the difference $\delta_{comp} - \delta_{free}$ for a given nucleus in order to evaluate the effect of complexation on these signals. It can be easily seen from this table that the *Ph*[19b]−N< carbon is the most affected carbon with a CIS value of 11.56 ppm. This CIS value is in line with CIS values (10−13 ppm) for carbons bound to deprotonated amines[33] [which are coordinated to vanadium(V)]. In marked contrast, the CIS value of −3.17 ppm (Table 7) for the carbonylic carbon of the −CON$^-$− functionality does not agree with the CIS value (11.9 ppm)[13b] obtained for the same type of carbon in a vanadium(V)−dipeptide complex recently reported[13b].

Infrared Spectroscopy. Assignments of some characteristic infrared bands are given in Table 8. Differences between the spectra of the ligands and vanadium complexes are readily noticeable. The ν(NH) bands are absent in the spectra of the complexes, as expected from the stoichiometry. Moreover, the amide II and III peaks are replaced by a medium to strong band at ca. 1335−1360 cm^{-1}. This replacement is to be expected, as the removal of an amide proton produces a pure C−N stretch.[35] The V = O stretching frequencies range from 983 to 961 cm^{-1}. The decrease in the vanadium oxidation state is reflected in a lowering of ν(V=O) {983 cm^{-1} for the complex **9** vs 961 cm$^-$ for its vanadium(IV) analogue}.

(34) Nugent, W. A.; Harlow, R. L. *J. Am. Chem. Soc.* **1994**, 116, 6142.
(35) Barnes, D. J.; Chapman, R. L.; Stephens, F. S.; Vagg, R. S. *Inorg. Chim. Acta* **1981**, 51, 155.

Table 8. Characteristic Infrared Bands (cm^{-1}) of the Ligands and their Vanadium Complexes.

	infrared bonds					
compound	ν(NH)	amide I[a]	amide II[b]	amide III[b]	ν-(V=O)	ν-(V−Cl)
Hcapca	3264 m	1677 s	1518 s	1271 m		
1		1632 s	1360 m			338 s
H_2phepca	3332 m	1689 s	1535s	1282 m		
2		1630 s	1355 s		983 s	
3		1628 s	1352 s		982 s	
H_3hypyb	3260 mb	1670 s, 1645 s	1520 s	1230s		
6		1629 s	1358 m		980 s	
H_4hybeb	3260 mb	1640 sb	1525 sb	1250 m		
7		1600 s	1345 s		961 s	
9		1602 s	1335 s		983 s	

[a] ν(C=O). [b] In secondary amides these bands arise from coupled ν(CN) and δ(NH) modes.

Table 9. UV-Visible Spectral Data for the Vanadium(III) and Various Oxovanadium (IV/V) Complexes

complex	λ_{max}, nm (ϵ,M^{-1}cm^{-1})[a]
1	451 (2700),[b] 322 (9000), 254 (sh) (11 500), 233 (sh) (12 500), 205 (22 500)
2	666 (sh) (27) 413 (10 800), 384 (sh) (9700), 302 (15 500), 261 (sh) (22 900), 234 (28 600)
3	635 (110), 390 (5600), 308 (10 900), 252 (22 000), 222 (23 000)
6	660 (sh) (39), 403 (sh) (2200), 307 (15 700), 255 (sh) (29 800) 224 (80 400)
7	650 (54), 521 (63), 317 (16 000), 254 sh (33 000), 227 (117 000)
$[VO(depa-H)]^{2-}$	610 (27)[b,c] 481 (sh), 294 (12 400)
9	600 (1950), 294 (sh) (24 800), 256 (sh) (33 000), 225 (85 200)

[a] In CH_2Cl_2. [b] In methanol. [c] Reference 9.

Electronic Spectra. Table 9 lists the spectral data for the vanadium(III) and various oxovanadium(IV/V) complexes. The visible absorption spectra of complex **1** [the vanadium(III) complex] and of complexes **2**, **3**, and **6** ($V^{IV}O^{2+}$ species) are dominated by an intense absorption ($\epsilon \geq$ 2000 M^{-1}cm^{-1}) at ∼400−450 nm and this band prevents the observation of the d−d transitions (except, of course, for a shoulder at ∼660 nm for complexes **2** and **6** and a band at 635 nm for complex **3**) expected for the d^2 (V^{III}) and d^1 (VO^{2+}) electronic configurations. In contrast complex **7** ($V^{IV}O^{2+}$ species) displays two low-intensity (ϵ∼60 M^{-1}cm^{-1}) d−d transitions at 650 and 521 nm. These bands are assigned[36] as $b_2(d_{xy}) \rightarrow e(d_{xz},d_{yz})$ and $b_2(d_{xy}) \rightarrow b_1(d_{x^2-y^2})$ transitions, respectively, assuming C_4v symmetry for this complex. It is worth noting that, its closely related complex {$[VO(depa-H)]^{2-}$},[9] which is also a bis[*N*-amidate−*O*-phenolate] $V^{IV}O^{2+}$ species, displays the $b_2 \rightarrow e$ and $b_2 \rightarrow b_1$ transitions at significantly lower energies (Table 9). The intense absorption in the visible region of the spectrum for complex **9**, the oxovanadium(V) species, can be assigned as ligand-to-metal charge transfer.

Electrochemistry. The results of the cyclic voltammetric and polarographic studies for the oxovanadium(IV) complexes in acetonitrile and dichloromethane are given in Table 10. The polarographic investigations in acetonitrile reveal one-electron reversible redox processes at −1.40, −1.21, −1.71, and −0.08 V for **2**, **3**, **6**, and **7** respectively, while in dichloromethane they show one-electron reversible redox processes at −1.44, −1.28, +0.56, and −0.16 V for the corresponding complexes.

The cyclic voltammetric examination of **6** and **7** in acetonitrile reveals the presence of two redox couples for the former and one redox couple for the latter. The peak separation (ΔE_p) for

(36) Ballhausen, C. J.; Gray, H. B. *Inorg. Chem.* **1962**, 1, 111.

Table 10. Electrochemical Data: Cyclic Voltammetric and Polarographic Studies of Oxovanadium(IV) Complexes[a]

complex	solvent	E_{pc},V	E_{pa},V	i_{pc}/i_{pa}	ΔE_p,[b] mV	$E_{1/2}$,[c] V	donor set[d]
2	CH_3CN	0.937	1.001	1.04	64	0.969	N_3O (−2)
		−1.387				(−1.40)	
	CH_2Cl_2	0.924	1.074	1.06	150	1.000	
		−1.536				(−1.44)	
3	CH_3CN	−1.21	−1.12	2.0	90	(−1.21)	N_3S (−2)
		0.84	0.95	0.5	110		
	CH_2Cl_2	−1.45	−1.15	1.8	300	(−1.28)	
			1.10				
6	CH_3CN	0.550	0.611	1.00	61	0.581	N_3O (−3)
		−1.737	−1.674	1.02	63	−1.706 (−1.71)	
	CH_2Cl_2	0.437	0.563	1.00	126	0.500 (0.56)	
		−2.0					
7	CH_3CN	−0.077	−0.016	1.00	61	−0.047 (−0.08)	N_2O_2 (−4)
	CH_2Cl_2	−0.229	−0.104	1.00	125	−0.167 (−0.16)	

[a] All potentials are relative to NHE. [b] $\Delta E_p = |E_{pc} - E_{pa}|$ at scan rate of 100 mV s^{-1}. [c] Values of the redox potentials ($E_{1/2}$) were calculated from the formula $E_{1/2} = 0.5(E_{pa} + E_{pc})$ from cyclic voltammetric measurements, while values in parentheses of the reduction potentials ($E_{1/2}$) were obtained from the intercepts of plots of $\log[(i_d - i)/i]$ vs potential (E). [d] The charge of the complexed ligand is given in parentheses.

each complex is close to that anticipitated for a Nerstian one-electron process (59 mV);[37] plots of C_p (peak current) versus $SR^{1/2}$ (SR = scan rate) are linear, and the ratio of the cathodic to anodic peak currents is 1, indicating that electron transfer is reversible and that mass transfer is limited. In dichloromethane one set of peaks is obtained for both complexes with peak-current ratios being unity and ΔE_p values being 126 mV for **6** and and 125 for **7** (ΔE_p for ferrocene under these conditions is 120 mV) and almost independent of scan rate below 500 mV s^{-1}, indicating that the redox processes are reversible (complex **6** reveals a cathodic peak at ca. −2.0 V as well). The two redox couples for **6** in acetonitrile have the same anodic and cathodic peak currents, indicating that both electrochemical processes have the same number of electrons, and since the redox couple at negative potentials is a one electron-process (polarography), the redox couple at the positive potentials must also be a one-electron process. All the other redox couples referred above are one-electron processes as well (polarography). Cyclic voltammetric studies of **2** in acetonitrile reveal one reversible couple of peaks (using the same reasoning as above) and a cathodic peak at −1.387 V, while in dichloromethane a couple of peaks with peak separation of 150 mV and a cathodic peak at −1.536 V are also obtained. Complex **3** revealed two irreversible couples of peaks in acetonitrile, while in dichloromethane it showed an irreversible couple of peaks at negative potentials and an anodic peak at positive potentials.

A blank cyclic voltammetric run of the ligands H_2phepca, H_3hypyb, and H_4hybeb in dichloromethane and acetonitrile as well reveals no redox activity in the potential range −1.0 to +1.3 V for both solvents and so it is concluded that the redox processes we observe at −0.047, 0.581, and 0.969 V in acetonitrile (Figure 6) and at −0.167, 0.500 and 1.000 in dichloromethane for the complexes **7**, **6**, and **2** respectively are metal based as illustrated for the complex anion $\mathbf{7}^{2-}$ in acetonitrile in eq 6. In contrast to the above mentioned redox

$$\mathbf{7}^{-} + e^{-} \rightleftharpoons \mathbf{7}^{2-} \qquad E_{1/2} = -0.047 \text{ V} \tag{6}$$

processes, owing to the metal center, we are unable to unequivocally assign the redox processes at −1.71, −1.40, and −1.21 V (these values are from polarography) in acetonitrile for the complexes **6**, **2**, and **3** respectively, to a V(IV) → V(III) reduction, as there is potential for reversible reduction of the complexed ligand, since the free ligand is reduced at ca. −1.4 (H_3hypyb) and −1.2 V (H_2phepca). In dichloromethane the neutral complexes behave similarly, while the reduction for the

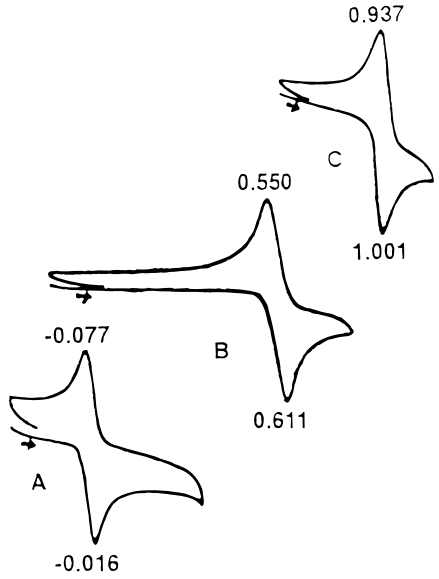

Figure 6. Cyclic voltammogram showing the oxidation of $V^{IV}O^{2+}$ to $V^{V}O^{3+}$ for the complexes **7** (A), **6** (B), and **2** (C), in acetonitrile/0.1 M Et_4NClO_4 at a platinum disk electrode with a scan rate of 100 mV/s.

complex anion $\mathbf{6}^{-}$ at ∼−2.0 V is very close to the reduction of the solvent and so we were unable to work out the number of electrons and the $E_{1/2}$ value for this redox process.

The cyclic voltammetric examination of **1** in acetonitrile shows a cathodic peak at −0.612 V and an anodic peak at +1.048 V. The ligand Hcapca exhibits, under the same conditions, two peaks at −1.617 and +1.583 V, while Et_4NCl shows an anodic peak at 0.960 V (which presumably is due to the oxidation of the chlorine). The anodic peak of the complex (1.048 V) can be assigned to the oxidation of the chlorine ligand, while the cathodic peak (−0.612 V) can be assigned to the reduction of vanadium(III) to vanadium(II).

It is of interest to note, that the reduction potentials ($E_{1/2}$) for the $V^{V,VI}O^{3+,2+}$ couple of complexes **2**, **6**, and **7** (Table 10; solvent CH_3CN) are very sensitive to the nature of the coordinating groups, spanning a range from ∼1.0 V to less than 0.00 V. A cathodic shift in the $E_{1/2}$ for the $V^{V,VI}O^{3+,2+}$ couple of ∼400 mV is found in substitution of the imino nitrogen ($phepca^{2-}$) for a deprotonated amide nitrogen ($hypyb^{3-}$), and an additional cathodic shift of ∼600 mV is observed in substitution of pyridine nitrogen ($hypyb^{3-}$) for a deprotonated phenolate oxygen ($hybeb^{4-}$). These differences in the $E_{1/2}$ values for the $V^{V,VI}O^{3+,2+}$ couple are due to (i) the difference in overall ligand charge (−2, −3, and −4 for $phepca^{2-}$, $hypyb^{3-}$, and $hybeb^{4-}$ respectively), (ii) the strong amido-N σ-donor

(37) Nicholson, R. S.; Shain, I. *Anal. Chem.* **1964**, 36, 706.

ability, and (iii) the strong affinity of the $V^{V}O^{3+}$ unit for phenolate oxygen.

Conclusion

The main conclusion of this study is that vanadium in its three most important biologically accessible oxidation states, namely III, IV, and V, forms strong bond(s) with the deprotonated amide nitrogen of the amide(peptide) functionality. The $V-N_{amide}$ bond length [mean $V-N_{amide} = 1.999(12)$ Å; Table 5] is almost independent of the oxidation state of vanadium-(III, IV, and V), geometry (octahedral−square pyramidal), and charge−donor set of the complexed ligand, −1 (N_4), −2 (N_3O, N_3S), −3 (N_3O), and −4 (N_2O_2).

The conclusion of this work is in line with excellent solution (water)[13b] studies concerning the reaction of vanadium(V) with small peptides, where the formation of a vanadium-deprotonated amide nitrogen bond is reported. The solid state (X-ray structures) and solution studies of interaction of vanadium with the amide (peptide) functionality provide evidence that $V-N_{amide}$ binding is a possible mode of action in proteins, though one has to be cautious, since the $N_{peptide}$ atoms in a protein are generally not as accessible as in a dissolved amide (peptide) molecule. Further studies concerning the reaction of vanadium with small peptides and amino acids are in progress in our laboratory.

Acknowledgment. Financial support from the General Secretariat of Research and Technology and John Boutari and Son Co. is gratefully acknowledged. We are indebted to Drs G. Varvounis (U. of Ioannina), J. Gallos (U. of Thessaloniki), S. Perlepes (U. of Patras) for helpful discusions and Mrs F. Masala as well for typing the manuscript of this paper.

Supporting Information Available: Tables listing atomic positional ($\times 10^4$) parameters of non-H atoms, positional and isotropic thermal parameters of the hydrogen atoms, anisotropic thermal parameters of the non-H atoms, bond lengths and bond angles associated with complexes **1**·CH_3CN, **3**, **4**·CH_3CN, **5**·$2CH_3OH$, and **10** (15 pages). Ordering information is given on any current masthead page.

IC9503803